International Conference "Water, Environment, Energy and Society" (WEES–2009)
New Delhi, 12–16 January 2009

Decadal Drought Analysis Using GCM Outputs

A.K. Mishra[1] and V.P. Singh[2]
Department of Biological and Agricultural Engineering, Texas A and M University
Scoates Hall, 2117 TAMU, College Station, Texas 77843–2117, USA
E-mail: [1]amishra@tamu.edu; [2]vsingh@tamu.edu

ABSTRACT: With increasing water scarcity around the world, exacerbated by drought incidences in terms of spatial and temporal variation along with the uncertainties associated with climate change, attention must focus on better understanding of different aspects of droughts. This paper discusses the impact of climate change on decadal drought severity and drought duration based on future climate scenarios derived from GCM outputs using downscaling techniques. It is observed that high drought severity and drought duration likely to be occurring for decades 2031–2040, 2041–2050, 2061–2070, and 2081–2090. The least drought decades are likely to be observed during 2021–2030 and 2081–2090. The observations were made based on short-term drought indices (SPI 1 and SPI 3).

INTRODUCTION

Droughts are considered by many to be the most complex but least understood of all natural hazards affecting more people than any other hazard. Droughts are a normal feature of climate and their recurrence is inevitable. However, there remains much confusion within the scientific and policy making community about their characteristics. Research has shown that the lack of a precise and objective definition in specific situations has been an obstacle to understanding droughts which has led to indecision and inaction on the part of managers, policy makers, and others (Wilhite *et al.*, 1986). Droughts have been recognized as one type of environmental disaster and have attracted the attention of environmentalists, ecologists, hydrologists, meteorologists, and so on. The global climate change in recent years is likely to enhance the number of incidence of droughts. While much of the weather that we experience is brief and short-lived, a drought is a more gradual phenomenon, slowly taking hold of an area and tightening its grip with time. In severe cases, a drought can last for many years, and can have devastating effects on agriculture and water supplies. Nearly 50 percent of the world's most populated areas are highly vulnerable to droughts. More importantly, almost all of the major agricultural lands are located there (USDA, 1994). Droughts produce a complex web of impacts that span many sectors of the economy and reach well beyond the area experiencing a physical drought.

Since almost one-half of the earth's terrestrial surface is susceptible to droughts, they are widespread phenomenon having significant social, economic, and environmental impacts. Human civilization has long been deeply affected by the impacts of droughts on economic, environmental, and social sectors (Wilhite, 1993). Only in the current decade large-scale intensive droughts have been observed on all continents. Droughts are the most costly natural disaster (FEMA, 1995; Wilhite, 2000; Svoboda *et al.*, 2002). Of all the 20th century natural hazards, droughts are those that have had the greatest detrimental impact (Bruce, 1994; Obasi, 1994). But droughts are not easily defined and need to be understood in terms of their hydrological, agricultural, and socio-economic impact (Dracup *et al.*, 1980; Wilhite and Glantz, 1985). Droughts impact both surface and groundwater resources and can lead to reductions in water supply, diminished water quality, crop failure, reduced range productivity, diminished power generation, disturbed riparian habitats, and suspended recreation activities, as well as a host of other economic and social activities (Riebsame *et al.*, 1991).

Due to population growth and expansion of agricultural and industrial sectors, the demand for water has increased in many parts of the world. Many other factors, such as climate change and contamination of water supplies, have contributed to water scarcity. The flood and drought events have been experienced with higher peaks and severity levels. The period between extreme events has been shortened in certain regions.

[1]Conference speaker

Lettenmiar *et al.* (1996) and Aswathanarayana (2001) have made references to this change in the occurrence of hydrologic extreme events. Decision makers and planners need to understand the impacts related to various levels of drought severity and the conditions that are associated with drought in order to take appropriate actions in the proactive management of water and other natural resources during droughts (Svoboda *et al.*, 2002; Wilhite, 2000a).

According to the Intergovernmental Panel on Climate Change (IPCC) report (IPCC, 2001), the surface temperature of the earth has risen steadily since the post-industry era of the 19th century. Sometimes it is stated that the most dangerous consequence of global warming is not the change in averages but the overall increase of extreme events. Among the extreme meteorological events, droughts are possibly the most slowly developing ones, that often have the longest duration, and at the moment the least predictability among all atmospheric hazards. Global warming, changes in precipitation patterns, and changes in resource use by humans in response to climate change could also significantly alter the quality of surface waters. While there is abundant evidence for dramatic and rapid climate warming in the past from lake-sediment, paleo-hydrology, and tree-ring records (Fritz, 1996; Ely *et al.*, 1993; Woodhouse and Overpeck, 1998; Murdoch *et al.*, 2000), never before have climate changes coincided with large-scale landscape fragmentation and alteration as is occurring today (Dale, 1997). It is very likely that the observed global warming has contributed to a change in rainfall patterns on a local or regional scale. Distribution of world agriculture shows adaptation to the present-day climate patterns, but this situation could change due to the likely global warming (IPCC, 2001). So, it is important to identify the water-scarcity periods, their severity, duration, and statistical behavior.

Recent climate changes have had a significant impact on the society. Some reports indicate that the mean annual global surface temperature has increased by about 0.3 to 0.6°C since the late 19th century and it is anticipated to further increase by 1–3.5° C over the next 100 years (IPCC, 1995). The Global Climate Models (GCMs) are generally used to simulate the present climate and project future climate with forcing by green house gasses and aerosols. GCMs, which describe the atmospheric cycle by mathematical equations, are the most adapted tools for studying the impact of climate change at regional scales.

This study aims to investigate decadal droughts in terms of their severity and duration. The Standardized Precipitation Index (SPI) (calculated from the probability distribution of precipitation using a two-parameter gamma function) was used as drought index. The SPIs were applied at the local scale using monthly rainfall data for the period of 1965–2001 from five raingauge stations in the basin. Using a Bayesian Neural Network (BNN) model, monthly rainfall values were simulated for the period 2000 to 2100. The basin is divided into 25 grid-cells of 13 × 13 km using Inverse Distance Weighting (IDW) approach, with each grid corresponding to approximately 4% of the total area for understanding the nature of droughts at each grid point. Finally, the decadal nature of drought severity and duration was assessed from the estimated gridded SPI values computed from precipitations based on GCM outputs.

STUDY AREA

The physical area considered in this study is the portion of the Kansabati River basin upstream of the Kangsabati dam, in the extreme western part of West Bengal state in eastern India. The region has an area of 4265 km^2. The elevation ranges from 110 m to 600 m above Mean Sea Level (m.s.l.). The average elevation of the region is approximately 200 m. The basin experiences very hot summer with the temperature in the region reaching up to 45°C in May and June. Generally, dry periods are accompanied by high temperatures, which lead to higher evaporation affecting natural vegetation and the agriculture of the region along with larger water resource sectors. The mean annual precipitation in the basin is about 1268 mm. Mainly three rivers contribute the flow in the Kansabati catchment, viz., Kansai, Kumari and Tongo. There is a dam called Kansabati dam constructed at the confluence of three rivers in Purulia district of West Bengal. The waters of the Kansabati dam are primarily used for irrigation. The major crops grown in the catchment are paddy, maize, pulses and vegetables.

The catchment is considered a drought prone area with irregular rainfall and the soils are mostly lateritic in nature having a low water holding capacity. About 50 to 60% of the study area is upland, which is managed by farmers generally with limited economic resources. Lands are mostly mono-cropped having limited surface irrigation facilities. The water demand due to the extensive cultivation has led to over exploitation of groundwater resources. The over-exploitation of groundwater, especially in summer has led to degradation of water resources. Irrigated crops are not widespread, because there is not always enough water available.

DATA USED

For this study, five raingauge stations were considered, as shown in Figure 1, and the statistical properties of rainfall series along with their geographic location are shown in Table 1. The mean annual rainfall varied from 1152.57 mm to 1345.7 mm during these years. The standard deviation for Phulberia station is quite high because of the high fluctuation of annual rainfall from a minimum of 674 to a maximum of 2081 mm. Since the basin is frequently affected by short-term droughts, it is necessary to investigate droughts in the basin. The basin was affected by severe droughts in the year 1965, 1966, 1967 and around the 1980's, the droughts were for a longer duration. The severity of a drought in 1990's was for a short period. The minimum rain gauge density for flat regions of temperate Mediterranean and Tropical zone is one station per 600–900 km^2 (according to World Meterological Organization), which seems reasonably adequate for the present study.

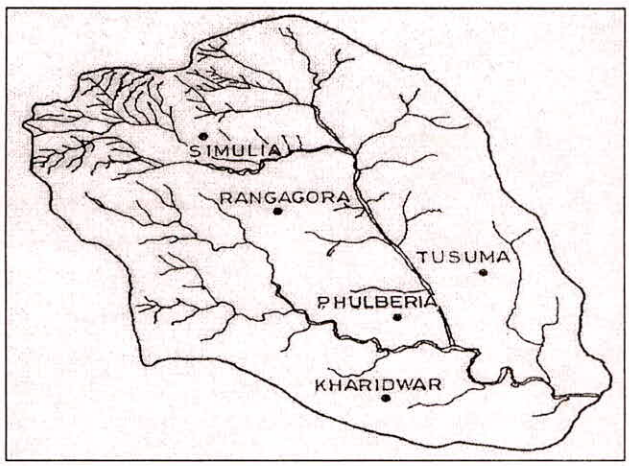

Fig. 1: Location of raingauge stations used in the study

Climate variables corresponding to the future climate change scenarios were extracted from the second version of the Canadian Centre for Climate Modelling and Analysis (CCCma), website http://www.cccma.ec.gc.ca/models/cgcm2.shtml. This simulation which was performed with the second version of the CCCma Coupled Global Climate Model CGCM2 with late 20th century concentration of CO_2. This model is based on the earlier CGCM1 (Flato *et al.*, 2000), but with some improvements to address shortcomings identified in the first version. In particular, the ocean mixing parameterization has been changed from horizontal/vertical diffusion scheme to the isopycnal/eddy stirring parameterization of Gent and McWilliams (1990), and sea-ice dynamics has been included following Flato and Hibler (1992). A description of CGCM2 and a comparison, relative to CGCM1, of its response to increasing greenhouse-gas forcing can be found in Flato and Boer (2001).

METHODOLOGY

Entropy

The concept of entropy has been popular in the scientific literature over the last several decades and has potential application to a range of problems in hydrology and water resources engineering (Singh, 1997). Shannon defined the entropy of a discrete time discrete alphabet random process {Xn}, denoted by H(X), as the amount of information in the process. Entropy, as defined in information theory, is a measure of uncertainty of a particular outcome in a random process, and provides an objective criterion in selecting a mathematical model. Uncertainty of two variables, X and Y, can be described by joint entropy $H(X, Y)$. The joint and marginal entropies are related as,

$$H(X, Y) = H(X) + H(Y) - T(X, Y) \qquad \ldots (1)$$

where $T(X, Y)$ is the information transferred from X to Y; called transinformation. Transinformation is a reduction of the original uncertainty, and it can be viewed as information about a predicted variable transferred by the knowledge of a predictor. In other words, Mutual information or Transinformation is a measure of the information contained in one process about another process, which is used in the present study for selecting predictors for downscaling experiments.

Table 1: Raingauge Stations in the Kansabati River Basin

Raingauge Stations	Elevation (m) (a.m.s.l)	Geographic Coordinates		Statistical Properties of Annual Rainfall Series (1965 to 2001)					
		Latitude	Longitude	Mean (mm)	Max (mm)	Min (mm)	Standard Deviation	Skewness	Kurtosis
Simulia	220.97	23° 10'	86° 22'	1300.68	1840	828	260.32	0.174	–0.605
Rangagora	222.92	23° 4'	86° 24'	1152.57	1729	743	219.1	0.782	0.656
Tusuma	158.6	23° 08'	86°43'	1268.3	1683	746	239.31	–0.221	–0.547
Kharidwar	135.96	23° 00'	86°38'	1216.97	1814	827	248.2	0.637	–0.306
Phulberia	144.32	22° 55'	86° 37'	1345.7	2081	674	322.73	0.329	–0.006

Artificial Neural Network (ANN)

The Back Propagation Network (BPN), developed by Rumelhart *et al.* (1986), is the most prevalent of the supervised learning models of Artificial Neural Networks (ANN). BPN uses a gradient steepest descent method to correct the weight of interconnective neurons. BPN easily solves the interaction of the processing elements by adding hidden layers. In the learning process of BPN, the interconnection weights are adjusted using an error convergence technique to obtain a desired output for a given input. In general, the error at the output layer in the BPN model propagates backward to the input layer through the hidden layer in the network to obtain the final desired output. The gradient descent method is utilized to calculate the weight of the network and adjusts the weight of interconnections to minimize the output error. In this paper an ANN using back propagation algorithm was used to simulate future monthly rainfall values.

Bayesian Neural Network (BNN)

The Bayesian approach is applied here because of its particular advantage compared with classical models. ANNs have been successfully used in rainfall-runoff modeling for more than a decade. Since its inception, many researchers (ASCE, 2000) demonstrated its capability in complex non-linear rainfall-runoff modeling. The main conclusions of those studies are that the artificial neural networks can be considered as a robust modeling tool alternative to conceptual and physically based hydrologic models. However, there are major limitations in the conventional neural network approach (Coulibaly *et al.*, 2001). One of the main limitations is that the network is trained by maximizing a likelihood function of the parameters or equivalently minimizing an error function in order to obtain the best set of parameters starting with an initial random set of parameters. Sometimes a regularization term with an error function is used to prevent overfitting. In this method, a complex model can fit the training data well but it does not necessarily mean that it will provide smaller errors with respect to new data. This happens because of not considering uncertainty about the model parameters or the uncertainty about the relationship between input and output mapped by the network during training. The Bayesian approach attempts to overcome that problem, and provides prediction with an uncertainty estimate in form of confidence intervals.

In the Bayesian approach, the uncertainty about the relationship between input and output is represented by a probability density function of the parameters. Before observing data, parameters are described by a prior probability density function, which is typically broad to reflect the fact that we have little idea of what values the parameters should be. Once the data are observed, using Bayesian theory the corresponding posterior probability density function is derived (Khan and coulibaly, 2006). The posterior distribution may be found narrower than the prior distribution because some values of the parameters are more consistent with data than others. Taking account of uncertainty in parameter estimation enables the network to predict more accurately, reducing the problem of overfitting while dealing with new data. Moreover, the posterior distribution over network weights will provide a distribution over the outputs of the network, which is known as predictive distribution for the new data. If a single-valued prediction is needed, one might use the mean of the predictive distribution but the full predictive distribution also tells how uncertain this prediction is. It has been shown in the work of Sarle (Sarle, 1995) that even the crudest Bayesian computation (maximizing over both parameters and hyperparameters) is capable to generalize better than early stopping when learning nonlinear functions. Furthermore, the overfitting problem can be solved by using Bayesian methods to control model complexity. In the Bayesian approach, cross-validation is not required, because Bayesian methods allow for the values of regularization coefficients to be selected using only the training data. A detailed description of the BNN as used herein can be found in Khan and Coulibaly (2006).

SPI

A drought index can be considered as a prime variable responsible for assessing the effect of a drought and quantifying different drought parameters. Common to all types of droughts is the fact that they originate from the deficiency of precipitation that result in water shortage for some activity or some group. As a result, practically all drought indices and drought definitions use this variable either singly or in combination with other meteorological parameters (WMO, 1975). The goal of a drought index is to provide a simple quantitative assessment of four drought characteristics, viz., severity, intensity, duration, and spatial extent.

The Standardized Precipitation Index (SPI) has been developed for the purpose of defining and monitoring droughts. A deficit of precipitation affects soil moisture, stream flow, reservoir storage, and ground water levels, etc. at different time scales. McKee *et al.* (1993) developed SPI to quantify precipitation deficits on

multiple time scales. Shorter or longer time scales may reflect lags in the response of different water resources to precipitation anomalies. SPI permits to determine the rarity of a drought or an anomalously wet event at a particular time scale for any location that has a precipitation record. A drought event is considered to occur at a time when the value of SPI is continuously negative and ends when SPI becomes positive. Table 2 provides a drought classification based on SPI. Some of earlier application of SPI can be referred to Mishra *et al.* (2007, 2008).

Table 2: Drought Classification Based on SPI

SPI Values	*Class*
>2	Extremely wet
1.5 to 1.99	Very wet
1.0 to 1.49	Moderately wet
–0.99 to 0.99	Near normal
–1 to –1.49	Moderately dry
–1.5 to–1.99	Severely dry
< –2	Extremely dry

Calculation of SPI: SPI is computed as follows (Guttman, 1999): (i) First, a probability density function that describes the long-term time-series of rainfall observations is determined. (ii) The base time of rainfall observation series can be any, depending on the time scale of interest. In the present study, running series of total precipitation corresponding to 3 months, 6 months, 9 months, 12 months, 24 months were used and as result the corresponding SPIs were calculated: SPI 3, SPI 6, SPI 9, SPI 12, SPI 24. (iii) Once the probability density function is determined, the cumulative probability of an observed precipitation amount is computed. (iv) The inverse normal (Gaussian) function, with zero mean and unit variance, is then applied to the cumulative probability distribution function, which results in SPI.

RESULTS AND DISCUSSION

Downscaling Experiment

The ANN and BNN model were used to downscale GCM outputs for the Kansabati basin. Monthly precipitation was used as predictant for the downscaling experiments. In this present study five stations with 37 years of rainfall data were used for downscaling. Climate variables corresponding to the future climate change scenarios were extracted from the second version of the Canadian Centre for Climate Modelling and Analysis (CCCma) Coupled Global Climate Model (CGCM2) data.

Selection of Variables

The selection of predictors is one of the most important steps in the downscaling experiment. Several attempts have been demonstrated in different parts of the world for identifying predictors. As the predictors vary from one region to another there are no general guidelines for the selection of predictors. In this study, predictor variables were screened using entropy as well as the coefficient of correlation. The predictors sharing the maximum information with the predictant were chosen for the downscaling experiment. The predictors having transinformation value above 0.25 were chosen as possible predictors.

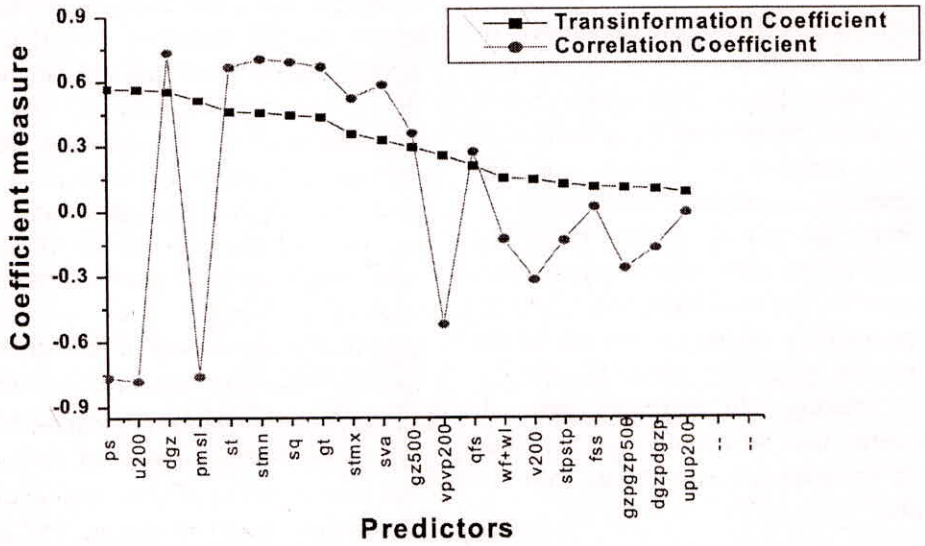

Fig. 2: Coefficient measures between predictants and predictors

The plots comparing trainsinformation and correlation coefficient are shown in Figure 2. The probable predictors selected for downscaling experiment include: Surface pressure (ps), 200 hPa wind velocity (u200), 500–1000 hPa Geop. Height (dgz), Sea Level Pressure (pmsl), Screen (2m) Temp (st), Mean Daily Min Screen Temp (stmn), Screen Spec. Humidity (sq), Skin (surface) Temp/SST (gt), Mean Daily Max Screen Temp (stmx), Mean 2m Wind Speed (sva), 500 hPa Geop. Height (gz500), 200 hPa V wind Variance (vpvp200). The variables chosen seemed physically sensible for downscaling in the study area.

Development of Neural Network Downscaling Model

The available data set was divided into a training set consisting of 70% of data and a testing set consisting of 30% of data. This model is a non-linear regression type in which a relationship is developed between a few selected large-scale atmospheric predictors and basin scale meteorological predictants. In setting up the standard Artificial Neural Network (ANN) model, a multilayer perceptron network has been used along with the input variables obtained based on entropy. Altogether 12 input vectors have been used to simulate precipitation. The above input variables have been found optimal in producing network outputs closer to the observed data, and providing the minimum Normalized Mean Square Error (NMSE) and the highest correlation coefficient.

For modeling BNN, the same Multilayer Perceptron (MLP) network has been used with the same set of input variables. The network architecture is similar to ANN, this includes one hidden layer with tangent hyperbolic (tanh) activation function and one output layer with linear processing unit. The trial and error approach has been used in network training based on the minimum NMSE and maximum CC. For simulation of precipitation with BNN, 10 neurons were found to be optimal in the hidden layer to obtain the best network. Unlike the standard ANN model, the initialization of the parameters in BNN is done using a distribution of parameters. The initial values of the weights and biases are obtained from a Gaussian prior distribution of zero mean and inverse variance a (also known as regularization coefficient or prior hyper-parameter). Gaussian prior has been chosen to favor small values for the network weights because a network with large weights will usually give rise to a mapping with large curvature (Nabney, 2004). Moreover, the Gaussian prior also provides computational simplicity. For prior hyperparameter a, a single initial value has been chosen for both hidden and output layer weights. In defining the objective function in the Bayesian framework, an error model for the data likelihood function is required. It is assumed that the target data is generated from a smooth function with additive zero-mean Gaussian noise. Thus, for the noise model, a Gaussian distribution with zero mean and constant inverse variance is used as defined in Khan and Coulibaly (2006). After defining prior and likelihood functions, the objective function has been set as posterior distribution of weights.

The network training is done by a trial and error approach as described above, and the network weights are optimized using the scaled conjugate gradients optimization technique to find the most probable weights (w_{MP}) by maximizing the posterior distribution of weights p(w|D) or it can be said by minimizing the error function S(w). The hyperparameters denoted by a and b, have also been optimized during training process using the evidence procedure (Bishop, 1995) in which hyperparameters are set to a value that maximize the evidence of the model p(D| a, b). Once the network has been trained, the simulations were carried out, in which posterior distribution has been approximated to Gaussian.

The ANN and BNN models initially were applied to test their capability for predicting monthly precipitation. Since yearly precipitation values are mostly concentrated in the monsoon period, the yearly time series were divided into three groups (i.e., March–June, July–October, November–February), and ANN and BNN were used to simulate the individual groups. The results of BNN model are shown in Table 3 and the plots of ANN and BNN models are shown in Figure 3. It is observed that BNN models are able to capture peaks better than ANN and hence used in the study for downscaling experiment.

Decadal Drought Analysis

After monthly rainfalls were downscaled to the grid level using GCM outputs, the monthly SPI values for each grid were calculated, based on time scales of 1 and 3 months, which are known as SPI 1 and SPI 3, respectively. These indices are used for short-term drought analysis (Mishra and Desai, 2005). Drought parameters, known as annual drought severity (sum of negative SPI values in dry spells) and annual drought durations for each station using run theory, were calculated. Two types of the threshold level was used for calculating drought parameters: (i) zero threshold was used to calculate drought severity and duration,

Table 3: Statistical Properties of BNN Simulated Results

Station Name		Observed		BNN Simulated			
		Mean (mm)	Stddev (mm)	Mean (mm)	Stddev (mm)	CC	NMSE
Simulia	Mar–Jun	119.56	122.34	86.3	70.28	0.70	0.56
	Jul–Oct	227.25	126.81	262.2	81.5	0.61	0.82
	Nov–Feb	8.78	10.96	18.18	11.53	0.55	1.12
Rangagora	Mar–Jun	85.06	105.01	82.35	61.83	0.80	0.3748
	Jul–Oct	216.42	128.11	229.7	63.35	0.52	0.85
	Nov–Feb	1.53	3.01	9.82	1.82	0.53	1.05
Tusuma	Mar–Jun	93.5	87.4	81.9	67.1	0.79	0.36
	Jul–Oct	196.5	92.38	277.2	79.6	0.60	0.98
	Nov–Feb	6.92	18.78	17.8	9.88	0.51	1.43
Kharidwar	Mar–Jun	91.83	110.85	75.48	64.54	0.75	0.49
	Jul–Oct	202.31	119.47	253.9	126.68	0.62	0.93
	Nov–Feb	15.1	29.26	9.21	17.31	0.59	1.01
Phulberia	Mar–Jun	91.56	103.4	84.01	62.63	0.72	0.49
	Jul–Oct	244.12	133.91	282.6	89.67	0.64	0.63
	Nov–Feb	17.93	35.69	13.01	18.54	0.55	1.11

which indicates all periods starting from 'near normal' to 'extreme dry' periods; (ii) the threshold of '–1' was used to calculate drought severity and duration indicating all periods starting from 'moderately dry' to 'extreme dry' periods. In order to compare the decades in terms of their drought severity and duration, the mean drought severity and duration for individual grids (consisting of 25 grids) were calculated for nine decades for period 2010 to 2100.

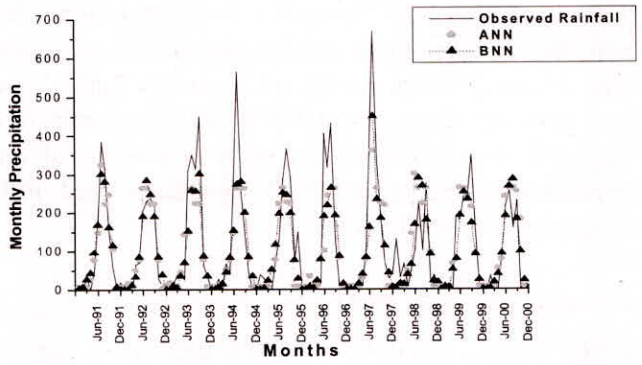

Fig. 3: Comparison between BNN and ANN for simulating monthly rainfall

The decadal drought severity based on SPI 1 using zero thresholds is shown in Figure 4. It can be seen from the figure that the drought severity for the period 2011–2020, 2021–2030 and 2081–2090 are less in comparison to other decades. For these periods the drought severity bands for all grids are close to each other, indicating uniform drought severity across the basin. The drought severity for 2041–2050 is high in comparison to 2031–2040, where the drought severity bands are clustered at a higher severity level except at a few grids. There is another interesting observation made for decade 2061–2070, indicating a mix drought severity for the basin. For this period nearly 50 percent area will be on a higher dry level and another 50 percent will be on a lesser dry level. In order to compare the decades with higher dry conditions, the decadal drought severity based on SPI 1 using –1 as threshold were calculated as shown in Figure 5. This threshold calculates all periods considering moderate dry to extreme drought conditions. It can be seen from the figure that the drought severity for period 2031–2040, 2041–2050 and 2071–2080 are on the higher side with severity bands clustered together indicating a uniform drought condition for the basin, where as for period 2061–2070, the basin undergoes a mixed condition of high and low dry conditions. Similar observations are made when SPI 3 is considered as a drought indice. The drought severity is likely to be high for period 2031–2040, 2041–2050 and a mix type condition for 2051–2060 and 2061–2070. The least dry conditions will likely to be observed during 2081–2090, followed by 2021 to 2030. Plots for SPI 3 are shown in Figure 6 and Figure 7.

The decadal drought duration based on SPI 1 using zero threshold is shown in Figure 8. It can be seen from the figure that the nature of drought duration is different from drought severity. The drought duration band seems to be more scattered in comparison to drought severity bands. The higher drought durations

likely to occur in the period 1941–1950. In order to compare the decades with higher dry conditions, the decadal drought duration based on SPI 1 using –1 as a threshold were calculated as shown in Figure 9. It can be seen from the figure that drought durations are highly random in comparison to drought severity. The bands of drought duration do not follow a regular pattern, with longest periods occurring around 1941–1950 and 2071–2080. Similar observations are made when SPI 3 was considered as drought indices (Figure 10). The drought duration seems to be in a mixed state, indicating nearly half of the grids following longer drought durations and the remaining shorter drought durations. These mixed conditions seem to be occurring for 2031–2040, 2041–2050 and 2071–2080. The least drought durations seem to be occurring in 2081–2090. When the –1 was used as a truncation level for SPI 3 (Figure 11), it was observed that the drought durations likely to be more during 2041–2050 and 2071–2080, where as the less drought duration period is likely to occur during 2021–2030 and 2081–2090.

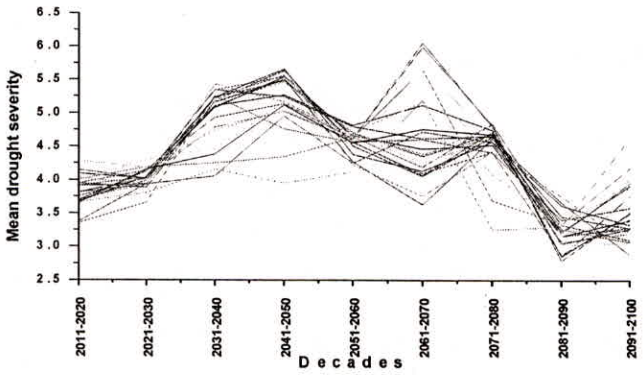

Fig. 4: Decadal mean drought severity for SPI 1 based on zero truncation level

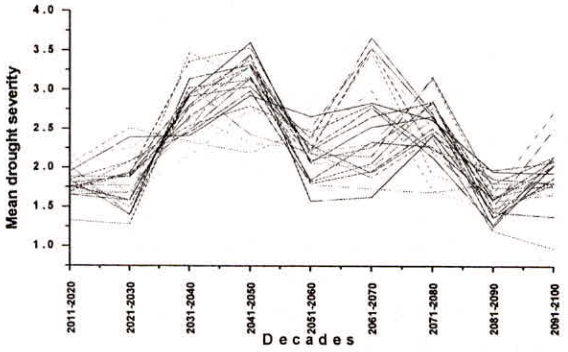

Fig. 5: Decadal mean drought severity for SPI 1 based on –1 truncation level

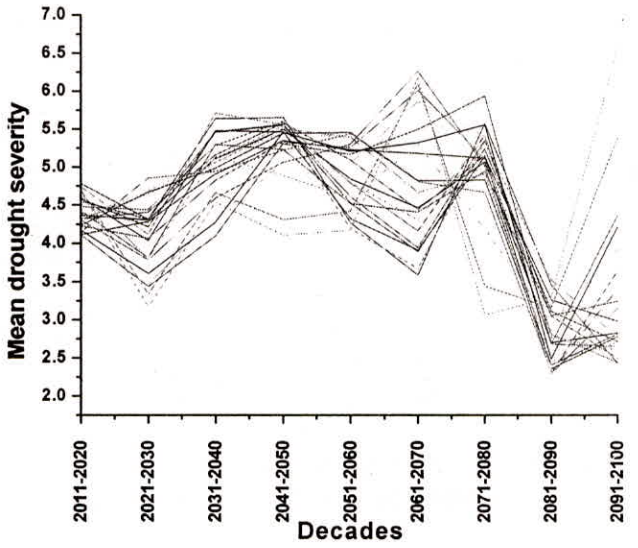

Fig. 6: Decadal mean drought severity for SPI 3 based on zero truncation level

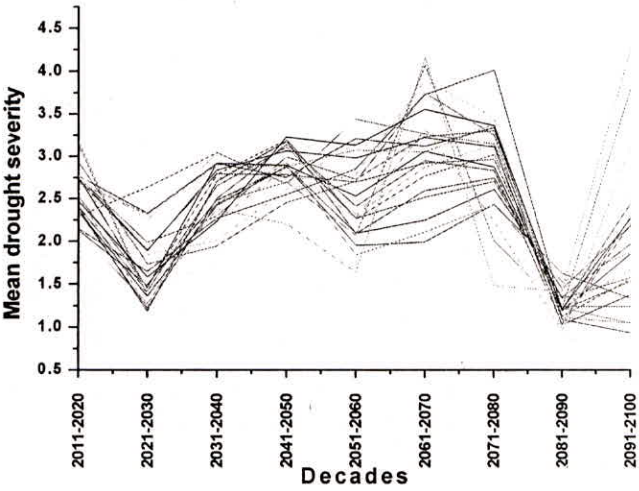

Fig. 7: Decadal mean drought severity for SPI 3 based on–1 truncation level

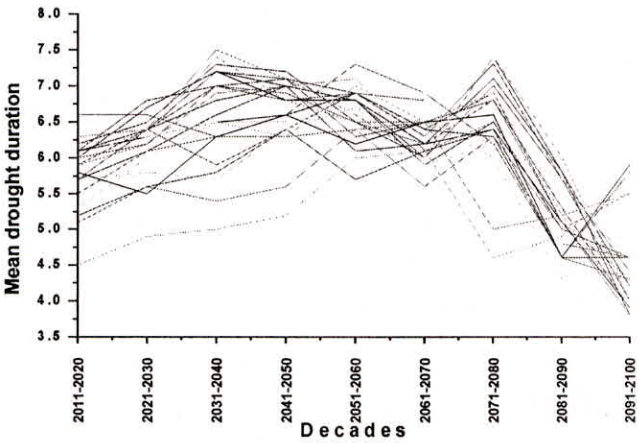

Fig. 8: Decadal mean drought duration for SPI 1 based on zero truncation level

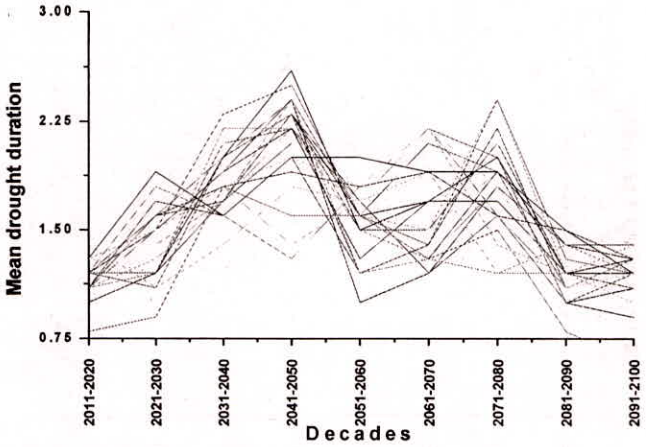

Fig. 9: Decadal mean drought duration for SPI 1 based on –1 truncation level

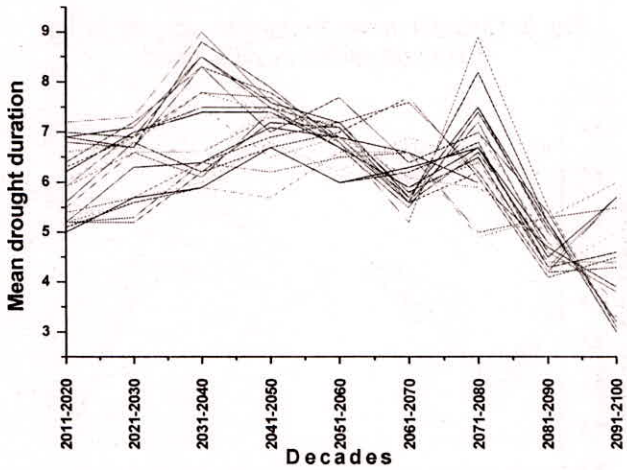

Fig. 10: Decadal mean drought duration for SPI 3 based on zero truncation level

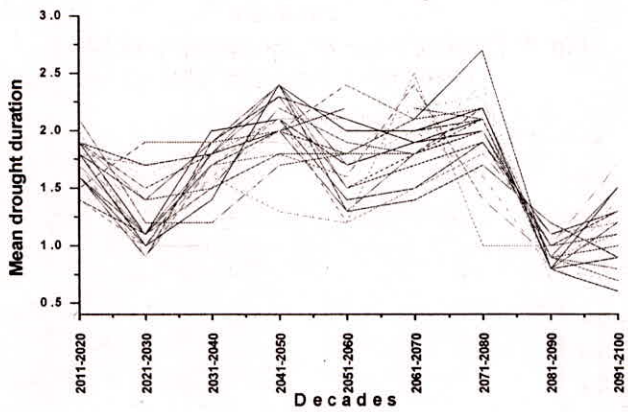

Fig. 11: Decadal mean drought duration for SPI 3 based on –1 truncation level

SUMMARY

The following conclusions can be drawn from this study:

1. Future projection of monthly rainfall is a key parameter in the present study. It is important to develop a proper downscaling model for assessing future scenarios. BNN seems to be performing better in comparison to the ANN model and the model needs to be calibrated carefully as it is highly sensitive to diffeerent inputs and model parameters.
2. As the choice of predictor variables can significantly affect the predictants in downscaling experiments because of highly spatio-temporal variability in hydrometeorological variables, it is important to identify suitable predictors. The entropy based approach for selecting the predictors seems to be an important development for down-scaling experiments.
3. Using GCM outputs, the projected decadal mean drought severity and drought duration will be useful for studying anticipated drought in future, in order to better prepare for water resources planning.
4. The high drought severity and drought duration likely to be occurring for decades 2031–2040, 2041–2050, 2061–2070, and 2081–2090. The least drought decades are likely to be observed during 2021–2030 and 2081–2090. The observations were made based on short-term drought indices (SPI 1 and SPI 3).

REFERENCES

ASCE Task Committee on Application of Artificial Neural Networks in Hydrology. (2000). "Artificial neural networks in hydrology. I. Preliminary concepts". *J. Hydrol. Eng.* 5(2), 124–137.

Aswathanarayana, U. (2001). *Water resources management and the environment*, Balkema, Rotterdam, The Netherlands.

Bishop, C.M. (1995). Neural Network for Pattern Recognition, Clarendon, Oxford, U. K.

Coulibaly P., Anctil F. and Bobee B. (2001). "Multivariate reservoir inflow forecasting using temporal neural networks", *J. Hydrol. Engg.* ASCE 6 (5), 367–376.

Dale, V.H. (1997). "The Relationship between Land-Use Change and Climate Change". *Ecological Processes* 7(3): 753–769.

Dracup, J.A., Lee, K.S. and Paulson, E.G. (1980). "On the statistical characteristics of drought events". *Water Resources Research* 16(2): 289–296.

FEMA (1995). National mitigation strategy: partnerships for building safer communities. Federal Emergency Management Agency, Washington, DC.

Flato, G.M. and Boer, G.J. (2001). "Warming Asymmetry in Climate Change Simulations". *Geophys. Res. Lett.*, 28, 195–198.

Flato, G.M. and Hibler, W.D. III. (1992). "Modelling Pack Ice as a Cavitating Fluid". *J. Phys. Oceanogr.*, 22, 626–651.

Fritz, S.C. (1996). "Paleolimnological Records of Climate Change in North America". *Limnology and Oceanography* 41(5): 882–889.

Gent, P.R. and McWilliams, J.C. (1990). "Isopycnal Mixing in Ocean Circulation Models". *J. Phys. Oceanogr.*, 20, 150–155.

Guttman, N.B. (1998). "Comparing the Palmer drought index and Standardized precipitation index", *J.of Amer. Water Resources Association.*, 34(1), 113–12.

IPCC (2001). In: Houghton, J.T., *et al.* (Eds.). Climate Change (2001). The Scientific Basis. Contribution of WGI to the Third Assessment Report of the Intergovernmental panel on Climate Change. Cambridge University Press, p. 881.

IPCC (1995). Impacts, Adaptations and Mitigation of Climate Change: Scientific-Technical Analyses, Cambridge University Press, UK, p. 878.

Khan, M.S. and Coulibaly, P. (2006). "Bayesian neural network for rainfall-runoff modeling". *Water Resources Research*, 42, W07409.

Lettenmiar, D.P., McCabe, G. and Stakhiv, E.Z. (1996). ''Global climate change: Effects on hydrologic cycle.'' *Water resources handbook*, Part V, Mays, L.W., ed., McGraw-Hill, New York.

McKee, T.B., Doesken, N.J. and Kliest, J. (1993). "The relationship of drought frequency and duration to time scales". *In Proceedings of the 8th Conference on Applied Climatology*, 17–22 January, Anaheim, CA. American Meteorological Society: Boston, MA, USA, 179–184.

Mishra, A.K. and Desai, V.R. (2005). "Spatial and Temporal Drought Analysis in the Kansabati River Basin, India" *International Journal of River Basin Management,* IAHR, 3(1), 31–41.

Mishra, A.K., Desai, V.R. and Singh, V.P. (2007). "Drought Forecasting Using a Hybrid Stochastic and Neural Network Model"; *J. Hydrologic Engg.* ASCE, 12(6), 626–638.

Mishra, A.K., Singh, V.P. and Desai, V.R. (2008). "Drought Characterization: A probabilistic approach", *Journal of Stochastic Environmental Research and Risk Assessment (Earlier Stochastic Hydrology and Hydraulics),* Springer Verlag, *(Published Online).*

Murdoch, P.S., Baron, J.S. and Miller, T.L. (2000). "Potential effects of climate change on surface-water quality in North America". *Journal of the American Water Resources Association*, 36(2), 347–366.

Obasi, G.O.P. (1994). ''WMO's role in the International Decade for Natural Disaster Reduction.'' *Bull. Am. Meteorol. Soc.*, 75(9), 1655–1661.

Riebsame, W.E., Changnon, S.A. and Karl, T.R. (1991). *Drought and Natural Resource Management in the United States: Impacts and Implications of the 1987–89 Drought.* Westview Press: Boulder, CO; 174.

Rumelhart, D.E., Hilton, G.E. and Willams, R.J. (1986). "Learning representations by back-propagating errors". *Nature* 323, 533–536.

Sarle, W.S. (1995). Stopped training and other remedies for overfitting, paper presented at the 27th Symposium on the Interface for Computing Science and Statistics, Carneigie Mellon University, Pittsburgh, Pa.

Shannon, C.E. (1948). "A mathematical theory of communication". *Bell Syst. Tech. J.*, 27:379–423,623–656.

Singh, V.P. (1997). "The use of entropy in hydrology and water resources". *Hydrological Processes,* 11, 587–626.

Svoboda, M. and Coauthors (2002). "The drought monitor". *Bull.Amer. Meteor. Soc.*, 83, 1181–1190.

USDA (1994). Major world crop areas and climatic profiles, World Agricultural Outlook Board, US department of Agriculture, Agricultural Handbook No. 664, pp. 157–170.

Wilhite, D.A. (2000). Preparing for drought: A methodology, in Drought: A Global Assessment, Routledge Hazards Disaster Ser., Vol. 2, edited by D.A. Wilhite, pp. 89–104, Routledge, Boca Raton, Fla.

Wilhite, D.A. and M.H. Glantz (1985). "Understanding the drought phenomenon: The role of definitions". *Water Int.*, 10, 111–120.

Wilhite, D.A. and Glantz, M.H. (1987). Understanding the drought phenomenon: the role of definitions. In: Wilhite, D.A., Easterling, W.E., Wood, D.A. (Eds.), Planning for Drought. Vestview Press, Boulder, CO, pp. 11–27.

Woodhouse, C.A. and Overpeck, J.T. (1998). "2000 Years of Drought Variability in the Central United States". *Bulletin of the American Meteorological Society* 79: 2693–2714.